# Formation of Supramolecular Structures between DNA and Starburst Dendrimers Studied by EPR, CD, UV, and Melting Profiles

**M. Francesca Ottaviani,*,† Farida Furini,‡ Angela Casini,‡ Nicholas J. Turro,§ Steffen Jockusch,§ Donald A. Tomalia,⊥ and Luigi Messori‡**

*Institute of Chemical Sciences, University of Urbino, Urbino, Italy; Department of Chemistry, University of Florence, Firenze, Italy; Department of Chemistry, Columbia University, New York, New York 10027; and Center for Biologic Nanotechnology, University of Michigan, Ann Arbor, Michigan 48109-0533*

*Received May 22, 2000; Revised Manuscript Received August 18, 2000*

ABSTRACT: Poly(amidoamine) starburst dendrimers (SBDs) form stable supramolecular structures (complexes) with DNA and confer protection against degradation by nucleases. Such properties make SBDs excellent candidates for application in gene delivery strategies. Formation of supramolecular structures by two generations of SBDs, namely 2SBD and 6SBD, with calf thymus DNA was examined at varying $r$ = [SBD](surface groups)/[DNA](base pairs) through various physicochemical techniques including electronic absorption spectroscopy (UV), circular dichroism (CD), DNA thermal denaturation studies (melting profiles), and electron paramagnetic resonance (EPR) spectroscopy. EPR spectroscopy of nitroxide-labeled dendrimers provides information on the interactions between SBDs and DNA, whereas the other techniques mainly monitor the structural variations of DNA following formation of SBD−DNA complexes. At the lowest $r$ values ($r < 1$), both dendrimers slightly affect DNA conformation within the general framework of B-type structure; minor stabilization effects of the double helix were detected through analysis of the melting profiles. When $r$ increases, extensive precipitation of the SBD/DNA adducts takes place due to charge neutralization effects. A persistent opalescence of the solution prevents recording of CD spectra up to $r = 100$ for 2SBD and $r = 200$ for 6SBD. However, at these $r$ values, EPR analysis indicates that a saturation of the interacting sites on DNA occurs which allows calculation of the formation constant of the SBD−DNA adducts. By further increasing the [SBD]/[DNA] ratio, DNA resolubilizes. At the high $r$ values, both SBDs form stable soluble supramolecular structures with DNA due to a "salting in" effect. EPR, CD, and UV results allow us to propose a model for the formation of different supramolecular structures in the various $r$ ranges.

## Introduction

Dendrimeric polymers are compact structures with high symmetry and well-controlled molecular properties, composed of layers of monomer units irradiating from a polyfunctional central core.[1] Among the dendrimers, the poly(amidoamine) starburst dendrimers (SBDs) are obtained by covalently attaching amidoamine units to an amino or ethylenediamine core.[2] The subsequent layers constitute the generations.[1,2]

Several applications of SBDs in biomedicine have been described. The internal structure and size of SBDs mimic biological macromolecules, including globular enzymes, viral proteins, antibodies, and, in particular, histones and polyamine such as spermine and spermidine.[2−4] Unlike other polymers, such as polylysines, SBDs are biocompatible and can be used in the pharmaceutical and biochemical fields as drugs and vehicles of biological materials,[5−8] as probes for oligonucleotide arrays,[9,10] and as primers in polymerase chain reactions (PCR).[9] SBDs have also been coupled to antibodies for application in immunoassays.[6] Notably, SBDs have been used as viral vectors and gene carriers to deliver DNA sequences in cells:[11] short DNA sequences can wrap around dendrimers and allow genetic material to be delivered to mammalian cells. SBDs are able to mediate the delivery of both natural and synthetic DNA or RNA of various kinds and sizes.[11] In vitro and in vivo transfection experiments involving SBDs have been carried out;[12,13] results indicate that the process is highly efficient and is strongly dependent on SBD generation, on the nature of target cells, and on the presence of other reagents such as DEAE−dextran.[14,15] Also, the cytotoxicity and the strength of Coulombic interactions between dendrimers and DNA are concentration and generation dependent: the higher generations (6SBD, 7SBD, 8SBD), although more cytotoxic, are more efficient in transfection compared with the lower ones.[3−8] DNA complexed by SBD is protected against degradation produced by specific nucleases.[5a,11]

To clarify some aspects of critical biological processes, such as gene transfection, it is essential to investigate, at a molecular level, the structure of host−guest SBD/DNA complexes, to obtain some insight into the supramolecular structures that might form. The first step in understanding the gene delivery and transfection processes is represented by the investigation of simple binary systems consisting of the dendrimers and the interacting biomolecule. Very recently, the electron paramagnetic resonance (EPR) technique has been employed to characterize the binary systems constituted by SBDs and liposomes, which mimic important properties of cell membranes.[16] In addition, EPR[17] and fluorescence[18] methods provide useful tools to investigate the interactions between SBDs and various polynucleotides.[17] Different interacting abilities toward the

† University of Urbino.
‡ University of Florence.
§ Columbia University.
⊥ University of Michigan.
* To whom correspondence should be addressed. Phone +0722-4164, fax +0722-2754, e-mail ottaviani@uniurb.it or ottavi@chim.unifi.it.

10.1021/ma000877i CCC: $19.00 
Published on Web 09/29/2000

**Scheme 1**

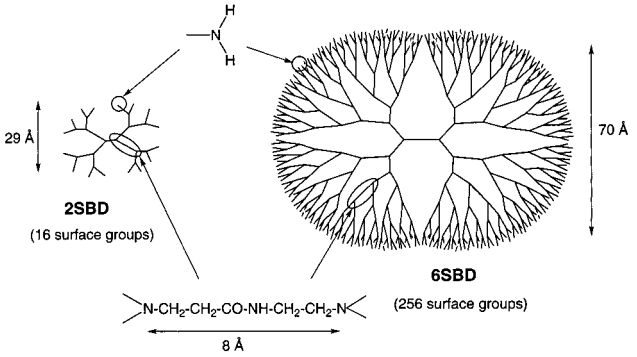


SBD surface were revealed by the different bases constituting the DNA sequence. These interactions were found to be mainly electrostatic in nature, although small dendrimers were demonstrated to interact with the DNA surface through less polar sites.

The present work aims at providing insight into the mechanisms of interaction between SBDs and DNA and structures of complexes formed between them. Information on SBD/DNA adducts was obtained using several techniques: EPR spectroscopy, in parallel with other physicochemical techniques (circular dichroism, UV−vis, and DNA melting profiles). To provide as much information as possible on SBD/DNA complex formation, the relative concentrations of SBD and DNA were varied systematically over a wide range, and the results were analyzed in terms of the ratio, *r*, between SBD concentration (in amino surface groups) and DNA concentration (in base pairs). To investigate the effects on complexation of differently sized dendrimers, we selected a prototype of the so-called "earlier generation" SBDs and one of the "later generation" SBDs, that is, 2SBD and 6SBD, respectively.[17]

For EPR studies, dendrimers were spin-labeled with a nitroxide radical (2,2,6,6-tetramethylpiperidine-*N*-oxyl), termed TEMPO. Henceforth, the labeled dendrimers were indicated as SBD-T. The TEMPO radical covalently linked to a few amino surface groups (about 3%) is very useful because it directly monitors the localization of the dendrimers in the vicinity of DNA surface as well as modifications of the interface properties due to dendrimer−DNA interactions.[16−18]

CD, UV spectroscopy, and melting profiles were applied to investigate conformational changes experienced by calf thymus DNA, when dendrimers−polynucleotide complexes are formed. Overall, these techniques follow the evolution of the system from the point of view of the nucleic acid structure and provide complementary data to the EPR technique.

## Experimental Section

**Starburst Dendrimers.** Poly(amidoamine) starburst dendrimers used in this work, indicated as *n*SBDs, where *n* is the generation, are characterized by an ethylenediamine core with terminal amino groups at the surface (Scheme 1). They were synthesized by published methods.[2]

**Circular Dichroism, Absorption Spectroscopy, and DNA Melting.** Each sample for CD, absorption spectroscopy, and DNA melting analysis was prepared by adding the required volume of a solution of either 2SBD or 6SBD, dissolved in a buffer (10 mM $NaH_2PO_4$, 100 mM NaCl), to calf-thymus DNA (Sigma Chemical Company) solutions. DNA concentration was determined measuring the UV absorbance at 260 nm ($\epsilon_M$ = 6600 $M^{-1}$ $cm^{-1}$). Typically, the DNA concentration was ~30 $\mu$g/mL corresponding to ~50 $\mu$M in base pairs. Samples were incubated at 298 K for 1 h. The range of [SBD](surface groups)/[DNA](base pairs) ratios (*r*) was varied between 0 and 800.

CD spectra were recorded on a Jasco J600 dichrograph interfaced with a PC and analyzed through the standard Jasco software package.

UV absorption spectra were recorded between 200 and 400 nm using a Perkin-Elmer Lambda 20 Bio spectrophotometer.

Thermal denaturation experiments were performed in quartz cuvettes with a Perkin-Elmer Lambda 20 Bio spectrophotometer. Samples were continuously heated with a rate of temperature increase of 0.5 °C/min while monitoring the absorbance changes at 260 nm. The investigated interval of temperatures ranged from 50 to 95 °C. Upon reaching 95 °C samples were cooled back to 40 °C in order to follow the renaturation process. Values for melting temperatures ($T_m$) and for the melting interval ($\Delta T$) were determined according to the reported procedures.[19] Differential melting curves (DMC) were obtained by numerical differentiation of experimental melting curves.[20]

**EPR Spectroscopy.** To investigate the adducts formed between SBDs and DNA via the EPR technique, the 2SBD and 6SBD dendrimers were spin-labeled with Tempo (2,2,6,6-tetramethylpiperidine-*N*-oxyl) nitroxide radicals. The latter were stored at 4 °C. The labeling procedure has been described elsewhere.[17] The label concentration is ca. 3% of the SBD surface groups. Labeled dendrimers will be signified to as *n*SBD-T. The EPR measurements were performed as a function of *r* = [SBD](surface groups)/[DNA](base pairs) at constant *n*SBD-T concentration (ranging from 0.005 to 0.04 M). Increasing amounts of calf-thymus DNA (Sigma Chemical Company) were added in order to obtain *r* ratios between 10 and 1000. To maintain a constant concentration of labeled dendrimers was necessary for a correct comparison of the various EPR results. However, EPR experiments carried out at constant DNA concentration and variable SBD-T concentration provided almost comparable results with respect to the results reported hereafter. Both DNA and SBDs were dissolved in a buffer consisting of 10 mM $NaH_2PO_4$ and 100 mM NaCl. Other samples were prepared in the absence of the buffer. In this case the natural pH of the dendrimer is about 9 for 6SBD-T and about 8 for 2SBD-T. Previous studies indicated that the amino groups at the surface are largely protonated (about 70%) at pH 9. Thus, in the buffered solution used in this study (pH 7.4) total protonation is expected.[22] The EPR spectra were recorded with a Bruker 200D spectrometer operating in the X band and interfaced through the Stelar software to a PC. The temperature was controlled with the aid of a Bruker ST 100/700 variable-temperature assembly.

## Results

**Circular Dichroism.** CD is undoubtedly one of the most powerful techniques for investigating the solution structure of DNA and the conformational modifications of the double helix produced by ligand binding. Although CD spectral changes cannot be interpreted on a quantitative theoretical basis, comparison of the experimental results with empirical spectra of representative DNA samples provides useful comparative and rather direct structural information. The effects of the addition of increasing amounts of 2SBD and 6SBD dendrimers on calf thymus DNA conformation were investigated in detail by CD spectroscopy in the UV. The intrinsic CD activity in the UV of each dendrimer, both labeled or unlabeled, was recorded and found to be negligible. The observed effects on the CD spectra produced by addition of increasing amounts of either labeled or unlabeled 2SBD to calf thymus DNA solutions are shown in Figure 1A−C.

Parts A and B of Figure 1 show the CD spectra of [2SBD]/[DNA] and [2SBD-T]/[DNA], respectively, at the various *r* values between 0 and 15. Figure 1C reports

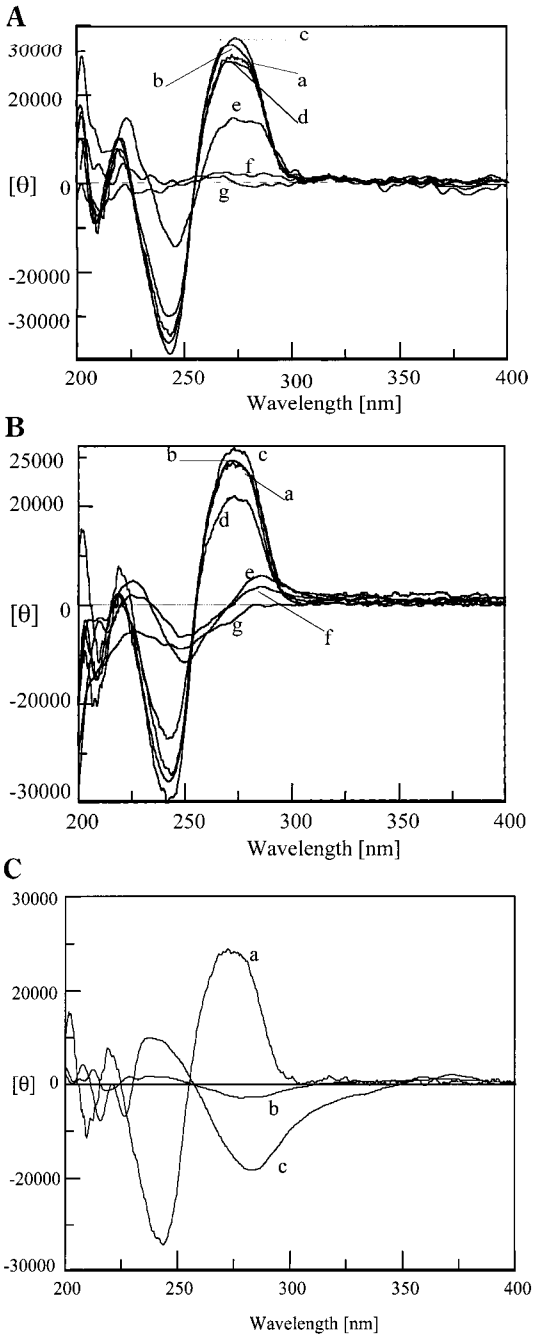


**Figure 1.** (A, B) CD spectra of 2SBD/DNA (A) and 2SBD-T/DNA (B) at various $r$ = [SBD](surface groups)/[DNA](base pairs)values: (a) $r = 0$; (b) $r = 0.005$; (c) $r = 0.05$; (d) $r = 0.5$; (e) $r = 1.5$; (f) $r = 5$; (g) $r = 15$. (C) CD spectra of 2SBD/DNAbp at (a) $r = 0$; (b) $r = 100$; (c) $r = 200$. DNA concentration is 30 $\mu$g/mL (50 $\mu$M in base pairs); $T$ = 298 K; 10 mM $NaH_2PO_4$ and 100 mM NaCl buffer, pH 7.4. The molar ellipticity [$\theta$] is expressed in units of deg $M^{-1}$ $cm^{-1}$.

the CD spectra of 2SBD at $r = 100$ and 200, also showing the $r = 0$ spectrum for comparison. At low [SBD]/[DNA] ratios ($0 < r < 0.5$) only minor effects on the B-type CD spectrum of calf thymus DNA are detected (Figure 1A); more precisely, addition of 2SBD produces a modest increase of the positive band at 270 nm and of the negative band at 240 nm (Figure 1A,B).

Labeled 2SBD-T (Figure 1B) produces somewhat stronger conformational effects than does unlabeled 2SBD. For example, at $r > 1$, 2SBD-T induces significant shifts in the position of the UV CD bands, not observed in the spectra of [2SBD]/[DNA] (Figure 1A). Notably, when 2SBD concentration causes [SBD]/[DNA] ratios to reach values of 1−1.5, extensive precipitation of DNA occurs. As a result of the precipitation of SBD/DNA adducts, the DNA concentration in solution decreases progressively (Figure 1A,B). In this concentration interval, the positive charges of the dendrimers roughly equal the negative charges of DNA so that charge neutralization occurs and leads to formation of insoluble adducts that precipitate from the solution. When the [SBD]/[DNA] ratio approaches 1, the residual CD signal of DNA is significantly perturbed (Figure 1A,B). For higher [2SBD]/[DNA] ratios, the CD signal disappears completely due to precipitation. However, by further increasing [2SBD]/[DNA] ratios, DNA is resolubilized. The precipitate is not visually apparent for $r >$ 10, but an observed opalescence of the solution indicates the presence of suspended material. In this region, no CD signal is obtained (Figure 1A). However, at higher ratios of [SBD]/[DNA], a CD signal reappears, as shown in Figure 1C. Furthermore, for $r > 100$, inversion of the sign of the CD bands at 240 and 270 nm is observed. (In Figure 1C, the sample with $r = 200$ provides an example of such behavior.)

CD titrations of calf thymus DNA with either labeled or unlabeled 6SBD are shown in Figure 2A−C. Figure 2A shows the CD spectra of [6SBD]/[DNA] at $r = 0-250$; Figure 2B shows the CD spectra of [6SBD-T]/[DNA] at $r = 0-250$; Figure 2C reports the CD spectra of 6SBD at $r = 0$ and several very high ratios >300. The spectra obtained with 6SBD and 6SBD-T almost coincide, in contrast to the situation for 2SBD and 2SBD-T for various values of $r$. Labeled SBDs at the lowest $r$ values (Figure 2B) produce smaller hyperchromic effects than do unlabeled SBDs (Figure 2A). Overall and qualitatively, the effects on the CD spectra produced by 6SBD resemble those of 2SBD but occur at larger $r$ values for 6SBD than for 2SBD. Indeed, at low ratios ($0 < r < 1$), 6SBD causes some hyperchromic effects on both the positive and the negative CD bands (Figure 2A,B). For 6SBD, DNA precipitation occurs over a very large concentration range: between $r = 1$ and $r = 40-50$ a gel precipitate is clearly visible in the solution. The CD signal is absent up to $r \sim 200-250$. Only at larger $r$ values (Figure 2C) does the CD signal reappear; at very high [6SBD]/[DNA] ratios ($r > 400$) dramatic hyperchromic effects on both CD bands are observed (Figure 2C), indicating the formation of soluble SBD/DNA supramolecular structures in the presence of a large concentration of this dendrimer.

**Electronic Absorption Spectra.** To confirm the picture emerging from the CD spectra and to quantify more precisely the amount of DNA present in solution following SBDs addition, absorption spectra in the UV were recorded for [SBD]/[DNA] solutions at varying $r$ values (Figure 3). Since SBD absorption at 260 nm is relatively low, reading of the absorbance at this wavelength provides direct information on DNA concentration in solution. On the other hand, for solutions of [SBD-T]/[DNA], the broad absorption band of the radical partially overlaps and interferes the absorbance of DNA, leading to an uncertainty in the analysis. Thus, we have only analyzed the absorption spectra obtained with unlabeled dendrimers.

In the case of 2SBD the characteristic UV band of DNA at 260 nm slightly increases in intensity even at the lowest $r$ values (Figure 3A); these changes closely correspond to the hyperchromic effects revealed by CD.

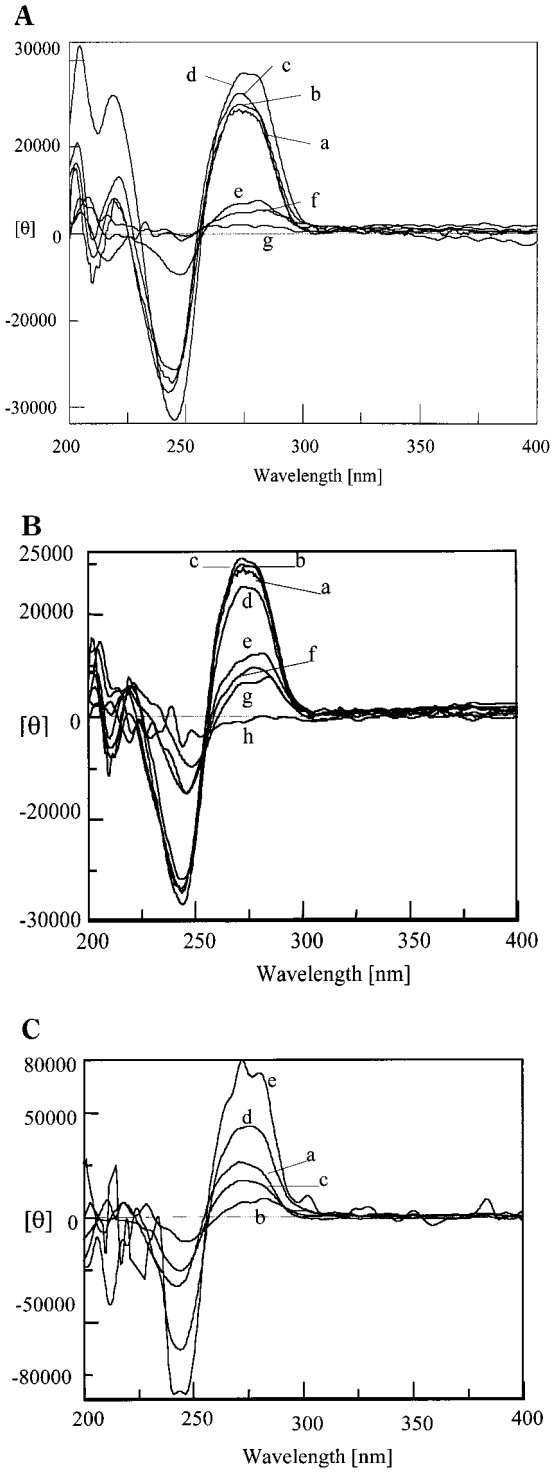


**Figure 2.** (A) CD spectra of 6SBD/DNA at various $r$ = [SBD](surface groups)/[DNA](base pairs): (a) $r = 0$; (b) $r = 0.025$ and $r = 1$; (c) $r = 0.25$; (d) $r = 0.8$; (e) $r = 2.5$; (f) $r = 8$; (g) $r = 25-200$. (B) CD spectra of 6SBD-T/DNA at (a) $r = 0$; (b) $r = 0.025$; (c) $r = 0.08$; (d) $r = 0.25$; (e) $r = 0.8$; (f) $r = 2.5$; (g) $r = 80$; (h) $r = 200$. (C) CD spectra of 6SBD/DNA at (a) $r = 0$; (b) $r = 300$; (c) $r = 400$; (d) $r = 500$; (e) $r = 800$. DNA concentration is 30 $\mu$g/mL (50 $\mu$M in base pairs); $T = 298$ K; 10 mM $NaH_2PO_4$ and 100 mM NaCl buffer, pH 7.4. The molar ellipticity $[\theta]$ is expressed in units of deg $M^{-1}$ $cm^{-1}$.

The observed spectral modifications are ascribed to minor conformational transitions induced by electrostatic interactions with the dendrimers. Upon approaching $r = 1$, a net decrease in the intensity of the 260 nm band is observed for dendrimers, directly related

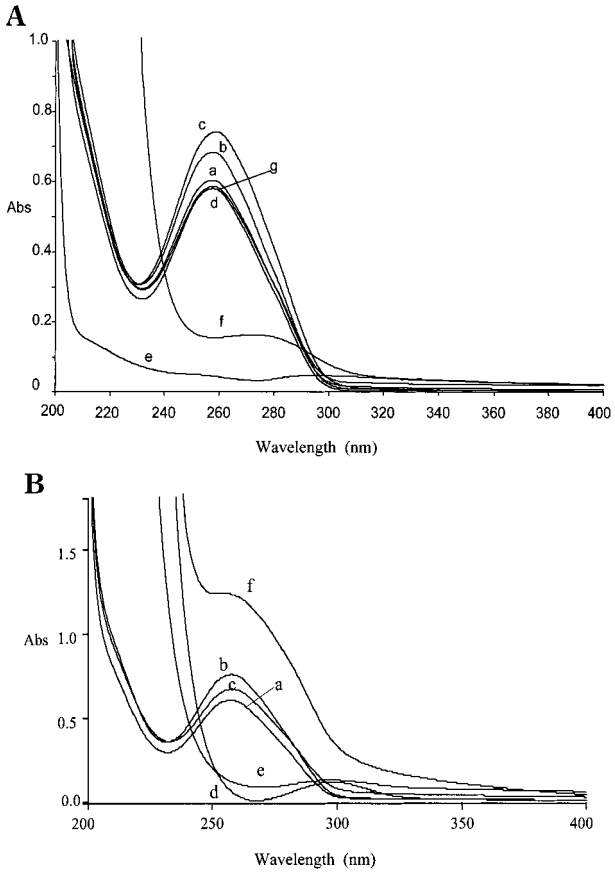


**Figure 3.** (A) UV spectra of 2SBD/DNA at various $r$ = [SBD](surface groups)/[DNA](base pairs): (a) $r = 0$, (b) $r = 0.05$, (c) $r = 0.1$, (d) $r = 0.5$, (e) $r = 1$, (f) $r = 200$ (g) $r = 500$. DNA concentration is 30 $\mu$g/mL (50 $\mu$M in base pairs); $T = 298$ K; 10 mM $NaH_2PO_4$ and 100 mM NaCl buffer, pH 7.4. For comparison purposes, the spectrum of 2SBD alone is shown in the inset (the concentration of surface sites is 0.01 M and corresponds to the concentration of the $r = 200$ adduct, trace f). (B) UV spectra of 6SBD/DNA at various $r$ = [SBD](surface groups)/[DNA](base pairs): (a) $r = 0$, (b) $r = 0.03$, (c) $r = 0.3$, (d) $r = 10$, (e) $r = 100$, (f) $r = 200$. DNA concentration is 30 $\mu$g/mL (50 $\mu$M in base pairs); $T = 298$ K; 10 mM $NaH_2PO_4$ and 100 mM NaCl buffer, pH 7.4. For comparison purposes the spectrum of 6SBD alone is shown in the inset (the concentration of surface sites is 0.01 M and corresponds to the concentration of the $r = 200$ adduct, trace f).

to DNA precipitation. At $r = 200$ a weak band becomes visible at higher wavelengths (about 275 nm) diagnostic of the fact that DNA starts being resolubilized. The intensity of this band slightly progressively increases as $r$ increases. At $r = 500$ the absorption spectrum matches closely the spectrum of pure DNA (trace g), indicating that DNA has been completely redissolved.

A similar behavior is observed for 6SBD (Figure 3B). At low $r$ values ($r = 0.03$ and $r = 0.3$) minor hyperchromic effects on the 260 nm band are detected. For higher $r$ values, for which massive DNA precipitation takes place (see trace d; $r = 10$), the absorbance of DNA is essentially absent. At $r = 100$ (trace e) the UV spectrum is still absent, but a sharp increase of the absorption signal occurs for $r = 200$ (trace f). In this case the band at 260 nm, appearing as a shoulder of a high-intensity band at $\lambda < 200$ nm, is assigned to redissolved DNA that is complexed with SBD. We shall demonstrate (vide infra) that at this $r$ value the EPR signal shows the maximum quenching in mobility, corresponding to a saturation of the DNA binding sites by the dendrimer.

**Table 1. Experimental $T_m$ and $\Delta T$ Values As Determined from the Thermal Denaturation Profiles; DNA Concentration Is 30 $\mu$g/mL (50 $\mu$M in Base Pairs)**

| | 2SBD | | | | |
|---|---|---|---|---|---|
| | $r = 0$ | $r = 0.0015$ | $r = 0.005$ | $R = 0.05$ | $r = 0.15$ |
| $T_m$ (°C) | 81.6 ± 0.5 | 81.7 ± 0.6 | 81.7 ± 0.5 | 81.8 ± 0.4 | 84.9 ± 0.5 |
| $\Delta T$ | 8.8 ± 0.6 | 8.6 ± 0.5 | 8.6 ± 0.4 | 8.7 ± 0.6 | 8.8 ± 0.6 |
| | 6SBD | | | | |
| | $r = 0$ | $r = 0.025$ | $r = 0.08$ | $R = 0.25$ | $r = 0.8$ |
| $T_m$ (°C) | 81.6 ± 0.5 | 82.0 ± 0.5 | 82.2 ± 0.5 | 83.1 ± 0.4 | 87.0 ± 0.5 |
| $\Delta T$ | 8.8 ± 0.6 | 8.4 ± 0.5 | 9.0 ± 0.6 | 8.9 ± 0.6 | 8.8 ± 0.6 |

Notably, the position of the UV signal for the 6SBD/DNA system moves to lower energies upon increasing $r$ up to 800 (data not shown).

**Melting Profiles.** To gain further insight into the effects on DNA conformation and stability produced by complexation of dendrimers, melting profiles were measured for SBD/DNA adducts at various $r$ values. The DNA melting technique directly monitors the changes of the thermal stability of the double helix following addition of DNA ligands which causes alterations of DNA structure.[19] Typically, DNA stability is largely enhanced when the ligand gives rise to electrostatic interactions with the phosphate groups of the double helix. Melting experiments were carried out in the low ratio range ($0 < r < 0.15$ for 2SBD and $0 < r < 0.8$ for 6SBD), the $r$ region just preceding adduct precipitation, and for some of the higher ratios. The results obtained at the lowest ratios are shown in Table 1. It is observed that addition of increasing amounts of the dendrimers results into modification and stabilization of the double helix, in line with the results from CD and UV measurements. For instance, the melting temperature ($T_m$) of calf thymus DNA increases by about 3 °C for 2SBD at $r = 0.15$ and by about 5 °C for 6SBD at $r = 0.8$. No significant changes of the melting interval $\Delta T$ were revealed in both cases (Table 1). The effects observed are in agreement with a simple electrostatic model of interaction. Notably, addition of the dendrimers, at the low ratios, does not favor DNA renaturation after melting. Far larger effects on the melting profiles are observed at the highest ratios; however, under these conditions the melting profiles are often dramatically perturbed and, therefore, are difficult to interpret. However, very complicated patterns of the dependence of absorbance at 260 nm on temperature are detected in agreement with formation of SBD/DNA supramolecular structures.

**EPR Analysis.** The EPR spectra at room temperature of the labeled dendrimers, 2SBD-T and 6SBD-T, display the usual three-line pattern due to the coupling between the unpaired electron spin and the nitrogen nuclear spin.[23] Although covalently linked to the dendrimer, the label possesses a certain freedom of motion. Addition of DNA causes a slight decrease in the height of the third line of the EPR profile, which is attributed to a reduction in the rotational mobility of the label resulting from binding of SBD-T to DNA.[24] However, the mobility remains in the range of fast motion. (The correlation time for the rotational mobility $\tau$ is $<2 \times 10^{-9}$ s.) This finding may seem to conflict in contrast with the occurrence of binding between the dendrimer and DNA, which should reduce the mobility of the labels. However, as shown in previous studies,[16b,17] other effects, e.g., the presence of a fraction of unbound dendrimers whose labels might mask the signal from the bound dendrimers, possibly contribute to the observed signals.

To avoid these interferences by unbound dendrimers, we performed EPR measurements at $T < 260$ K, below the freezing temperature of the samples. The samples were directly inserted in the EPR cavity kept at a fixed temperature. The freezing of a portion of the labeled dendrimers was quantified on the basis of the decrease in signal intensity. Under these conditions, a fraction of dendrimers, nonbound to DNA, separates from the solutions, and its EPR signal is too broad to be detected. In contrast, a fraction of the dendrimers in the vicinity of the DNA surface gives rise to a "glass transition", and the corresponding EPR signal indicates a progressive slowing of mobility with decreasing temperature. For this fraction of labels—about 30−40% of the initial amount (which is constant in most of the presented experiments)—the stronger the interaction with DNA, the lower the mobility of the labels at the DNA surface. EPR measurements were carried out by directly inserting the samples in the EPR cavity kept at 258 and 248 K; these temperatures were selected to enhance the differences (in mobility conditions) among the different systems studied in this work. Further measurements were carried out by progressively decreasing the temperature, but no additional information was obtained.

Figure 4 shows examples of experimental EPR spectra of [2SBD-T]/[DNA] (Figure 4A) and [6SBD-T]/[DNA] (Figure 4B) at 248 K at different $r$ ratios. Figure 4A also shows the $A_{zz}'$ component of the hyperfine coupling tensor $A$ (for the coupling between the electron spin and the nitrogen nuclear spin).[23] $A_{zz}'$ increases with the decrease in the mobility of the labels, thus indicating the stronger interaction and binding of the dendrimers with the DNA sites. This component was evaluated directly from the spectrum as shown in the figure. Figure 4B also shows the "slow" and the "fast" spectral components which constitute the EPR signals of 6SBD-T/DNA (where "slow" (s) and "fast" (f) are indicative of the mobility of the label). The subtraction of one component (obtained from 6SBD-T water solutions by changing temperature) from the overall EPR signal and the subsequent double integration of the two extracted components allow calculation of the $I_s/I_f$ parameters: $I_s/I_f$ represents the intensity ratio between "more interacting" (in close contact with DNA sites) and "less interacting" (i.e., in the vicinity of the DNA surface) labels, characterized by different mobility conditions. It must be stressed that while the spectra of 6SBD-T/DNA are constituted by both components, the spectra of 2SBD-T/DNA showed only the "stronger interacting" component, for which only the $A_{zz}'$ parameter is evaluated.

The $A_{zz}'$ and the $I_s/I_f$ parameters, evaluated for 2SBD-T/DNA and 6SBD-T/DNA systems, are plotted as a function of $r$ in Figure 5. First of all, it must be noted that the data from 2SBD-T samples are evaluated at 258 K, whereas the data for 6SBD-T are obtained at 248 K. Indeed, to obtain similar mobility conditions of the more interacting component, 6SBD-T needed a lower temperature (248 K) with respect to 2SBD-T (258 K). The plots show the occurrence of multiple maxima and minima. Maxima are assumed to correspond to the saturation binding of the "interacting sites" on the DNA surface by the dendrimers, whereas minima indicate loss of saturation. It is significant that more than one saturation condition is met upon increasing $r$ within the range 10−1000.

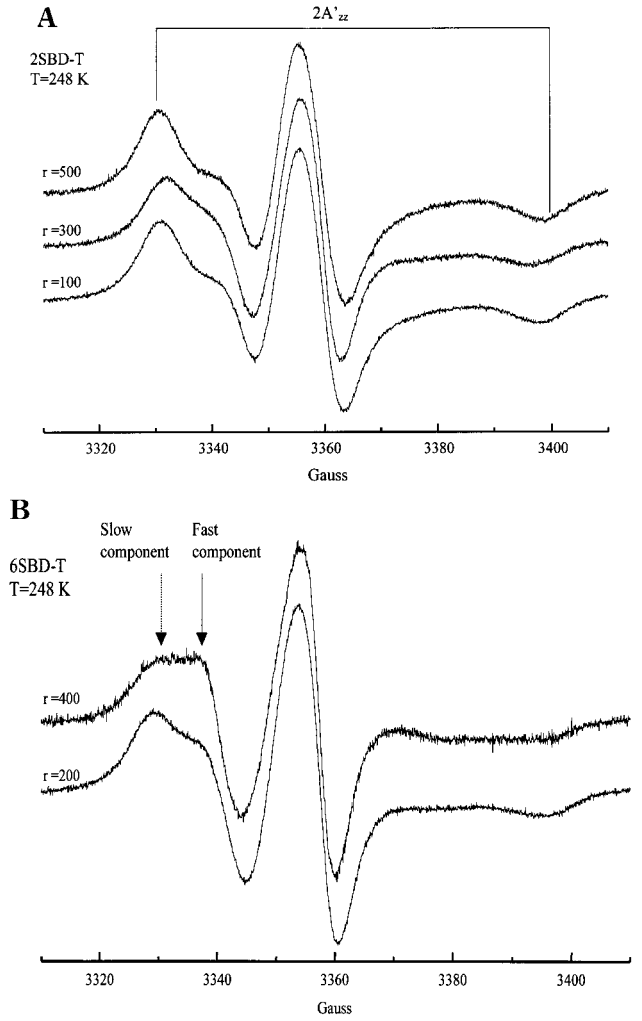


**Figure 4.** Experimental EPR spectra of 2SBD-T/DNA (A) and 6SBD-T/DNA (B) at 248 K and at different $r$ = [SBD](surface groups)/[DNA](base pairs). Constant SBD concentration in surface groups = 0.01 M.

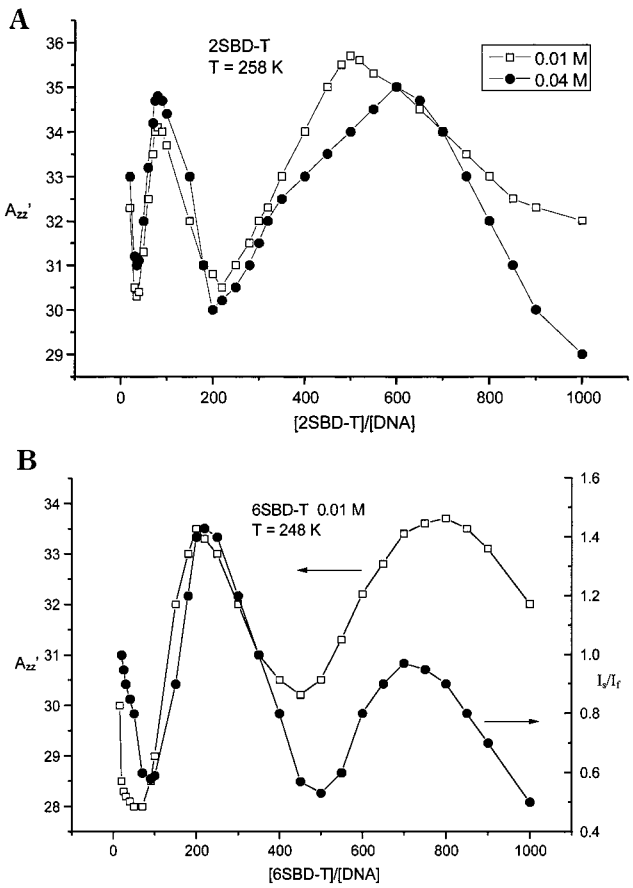


**Figure 5.** (A) Plot of $A_{zz}'$ as a function of $r$ = [2SBD-T](surface groups)/[DNA](base pairs) at $T$ = 258 K and two fixed 2SBD-T concentrations: 0.01 M (open squares) and 0.04 M (full circles) in phosphate buffer solutions. (B) Plot of $A_{zz}'$, extracted from the interacting component in the EPR spectra (open squares), and $I_s/I_f$ (full circles) as a function of $r$ = [6SBD-T](surface groups)/[DNA](base pairs); EPR spectra recorded at $T$ = 248 K and at a fixed SBD concentration of 0.01 M in phosphate buffer solution.

Considering the data in more detail, the plot obtained for 2SBD-T (Figure 5A) starts from $r = 10$. Data at lower $r$ values could not be collected due to intrinsic limits in the solubility of the SBD/DNA adducts and in the sensitivity of the technique. Upon increasing $r$ a progressive decrease in $A_{zz}'$ is observed until a sharp minimum is reached for $r$ values around 40. At larger $r$, $A_{zz}'$ increases until it reaches a sharp maximum at $r \approx 100$. Moving to higher $r$ values, $A_{zz}'$ decreases again and reaches a second minimum at $r \approx 200$. Further increases in $r$ cause an increase in $A_{zz}'$ once more to provide a second broader maximum at $r \approx 500$. It was found that the second maximum is shifted toward higher values when working at 0.04 M (surface groups) SBD concentration (instead of 0.01 M). For larger $r$ values ($r > 600$), $A_{zz}'$ decreases again. Values larger than 1000 are not reported, since the mobility increases and approaches that obtained for pure SBD solutions (unbound dendrimers).

In the case of 6SBD-T a qualitatively similar pattern of maxima and minima is observed for the dependence of both $I_s/I_f$ and $A_{zz}'$ on $r$ (Figure 5B). However, the first peak centered at $r \approx 200$ is broader than in the case of 2SBD-T, and the maxima are shifted toward higher $r$ values with respect to 2SBD-T. Also, the broad maximum at the highest $r$ values is slightly different depending on the measured parameter; it is at $r \sim 700$ for $I_s/I_f$, whereas it increases at $r \sim 800$ for $A_{zz}'$.

Remarkably, the EPR parameters of both 2SBD-T and 6SBD-T in the absence of the buffer are completely different. As shown in Figure 6, a true saturation curve is found, reaching a plateau at $r \sim 700$ and then slightly decreasing at high $r$ values. Again, the spectra of 2SBD-T allow calculation of $A_{zz}'$, since only the "strongly interacting" component was observed, whereas the main parameter for 6SBD-T, which provides information on the interaction with DNA, is $I_s/I_f$. In this case the parameters of both 2SBD-T and 6SBD-T are evaluated at $T$ = 258 K; the intensity ratio $I_s/I_f$ for 6SBD-T at saturation is particularly high, also at $T$ = 258 K, in comparison with the buffered solutions. The plot of $A_{zz}'$ for 2SBD-T starts at $r$ = 300, since at lower $r$ values the spectra show fast motion. ($A_{zz}'$ could not be evaluated.) The absence of the first broad maximum and the saturation at higher $r$ values may be caused by the basicity of the dendrimer solutions; in the absence of the buffer, the pH of the dendrimer solutions is about 8−9, and this prevents neutralization of DNA phosphate groups by SBDs. Thus, the formation of a precipitate and of the opalescence at the intermediate $r$ values are impeded.

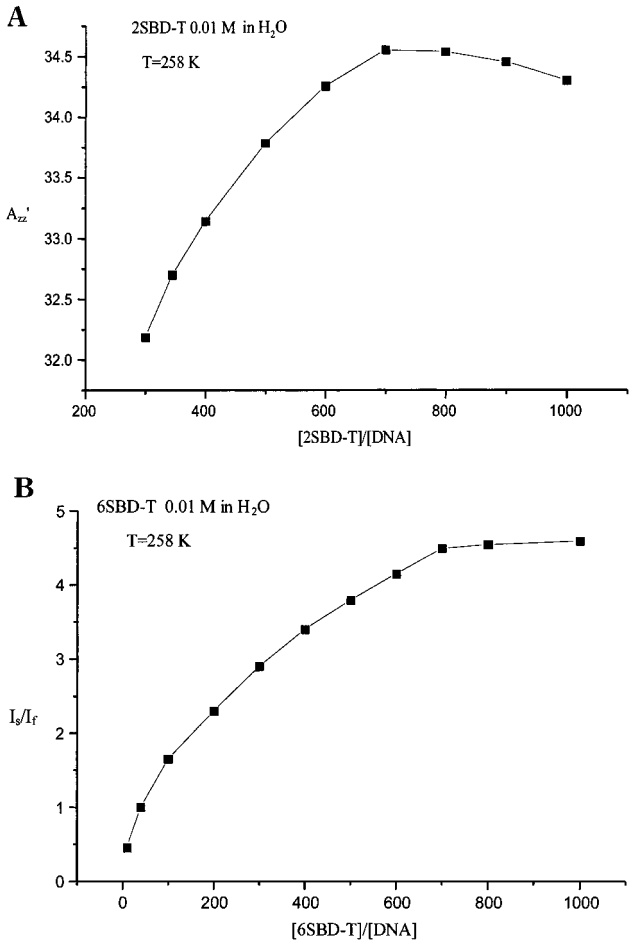


**Figure 6.** (A) Plot of $A_{zz}'$ as a function of $r$ = [2SBD-T](surface groups)/[DNA](base pairs): EPR spectra recorded at $T$ = 258 K and at fixed 2SBD-T concentration of 0.01 M in water. (B) Plot of $I_s/I_f$ as a function of $r$ = [6SBD-T](surface groups)/[DNA](base pairs): EPR spectra recorded at $T$ = 258 K and at fixed 6SBD-T concentration of 0.01 M in water solutions.

## Discussion

The application of various physicochemical techniques to describe the interactions in solution between two starburst dendrimers, 2SBD and 6SBD, and calf thymus DNA has provided considerable information on the structure and interactions of SBD/DNA complexes. EPR, UV, and CD spectroscopies and DNA melting profiles supply a number of independent data on SBD/DNA complexes as a function of $r$. In some cases information provided by the individual techniques are complementary. Because of intrinsic sensitivity problems, the EPR technique covers only the region with $r > 10$. On the other hand, precipitation of SBD/DNA adducts (opalescence of the solution affects the results from ca. $r \sim 1$ up to $r = 200$) prevents the acquisition of melting profiles and CD and also modifies UV spectra within this interval. However, on the grounds of the information gained from the different techniques, it is possible to propose a general model for the structures and the interactions occurring in solution between SBDs and calf thymus DNA, in the relevant $r$ ranges. The model is based on the experimental results from this work and on results from a previous investigation[18] of the interactions of SBDs and DNAs. The main features of this model are summarized in Scheme 2.

The model comprises three well distinct phases depending on the $r$ ratio of SBD sites to DNA base pairs: (a) low $r$ ratios, (b) intermediate $r$ ratios, and (c) high $r$ ratios.

**Scheme 2**

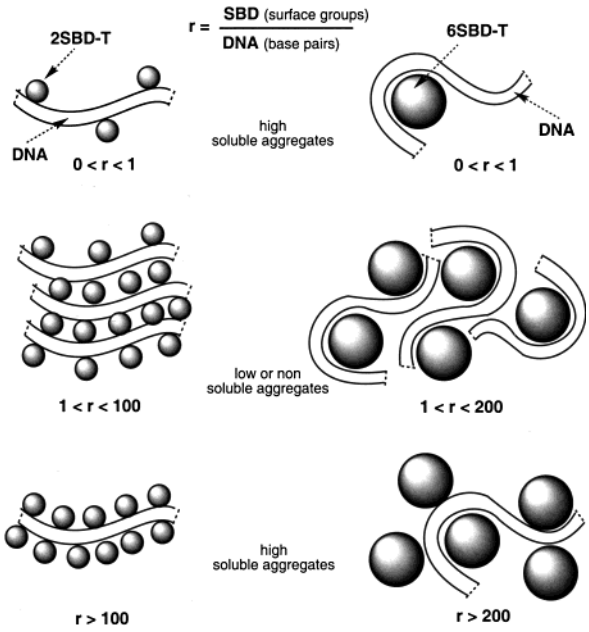


**(a) Low $r$ = [SBD]/[DNA] Ratios.** In the range of low $r$ values (defined as $r < 1$ for both dendrimers), the interactions of SBDs with calf thymus DNA are easily monitored through CD and UV absorption spectroscopies and DNA thermal denaturation profiles. CD results show that even at the lowest ratios both dendrimers produce small but significant changes of the characteristic B-type CD spectrum of DNA; the observed spectral modifications are diagnostic of binding to the double helix. In more detail, it is observed that both 2SBD and 6SBD cause a net hyperchromic effect on the positive band at 270 nm. Such effects are detected up to $r$ values ~0.8. Apparently, the small 2SBD dendrimer is more effective than 6SBD in modifying DNA conformation.

Overall, the significant CD changes at low $r$ values indicated that low concentrations of dendrimers are effective in reversibly perturbing the overall conformation of DNA, providing indirect evidence for tight binding. Furthermore, the modulation of the CD effects as $r$ increases is accounted by the different binding sites at the DNA surface, characterized by different binding affinities toward the few SBD molecules. For instance, the first addition of 2SBD in Figure 1A (trace b) produces larger spectral changes than the subsequent addition of a 10-fold amount (trace c), implying the presence of primary binding sites on DNA with higher affinity and larger conformational effects. The picture emerging from CD is confirmed by UV spectra showing significant hyperchromic effects at 260 nm even at the lowest SBD concentrations. DNA thermal denaturation profiles show some significant stabilization of the DNA double helix for $r$ values of 0.15 (2SBD) and 0.8 (6SBD); it turns out that 2SBD is more effective than 6SBD in stabilizing the double helix. For lower $r$ values melting parameters are scarcely affected by dendrimer addition, suggesting substantial preservation of double-helix native conformation. Renaturation profiles show that both SBDs do not favor the DNA renaturation process after melting, in agreement with the formation of stable DNA−SBD adducts in this range of $r$. These adducts are described as supramolecular structures in Scheme

2, in which few dendrimers are interacting with the DNA surface, being the large dendrimers partly wrapped up by the DNA strands.[18]

**(b) Intermediate *r* Ratios.** An intermediate range of values of $r$ (defined as $r > 1$ to ca. 100 for 2SBD and $r \sim 1$ to ca. 200 for 6SBD) is notable for the precipitation of SBD/DNA complexes that occurs due to charge neutralization effects. Apart from direct observation of the turbidity of the solutions and, at the lower intermediate $r$ values, of the formation of a gel precipitate, CD spectroscopy reports the progressive disappearance of the characteristic DNA signal in the UV for both dendrimers. For the purpose of the present study, the range of $r$, in which the formation of DNA/SBD aggregates at low solubility occurs, is well accounted for by the disappearance of the band at 260 nm upon passing from $r = 0.5$ to $r = 1$ for 2SBD and upon passing from 0.3 to 10 for 6SBD (see Figure 3). In turn, CD and UV also account for resolubilization of the DNA/SBD aggregates in the range 100/200 for 2SBD and 200/500 for 6SBD.

Centrifugation of the solutions containing a SBD-T/DNA gel precipitate provides a pellet whose EPR indicates that the mobility of the labels is strongly quenched (spectra not shown), whereas the supernatant solution exhibits a largely reduced EPR signal. Formation of the gel and subsequent opalescence of the solution most likely correspond to neutralization of the DNA negative charges with the positive charges of the dendrimer and to formation of large SBD/DNA aggregates, as shown in Scheme 2. The EPR results also account for the formation of such large aggregates. From $r = 10$ to $r = 40$ for 2SBD-T and to $r = 60-80$ for 6SBD-T, the $A_{zz}'$ and $I_s/I_f$ parameters decreased (increase in mobility) down to a minimum, since the system is reorganizing from the saturation of the sites in the single DNA strands to formation of aggregates constituted by various DNA and SBD molecules. When the mobility begins decreasing after the minimum, the formation of the large low-soluble aggregates shown in Scheme 2 prevails. The increase in the EPR parameters $A_{zz}'$ and $I_s/I_f$ continued approaching the $r = 100$ and $r = 200$ maximum conditions, for 2SBD-T and 6SBD-T, respectively.

**(c) High *r* Ratios.** Soluble SBD/DNA adducts were formed at high $r$ values (defined as $r > 100$ for 2SBD and $r > 200$ for 6SBD). Indeed, addition of large amounts of both SBDs ($r > 100$ for 2SBD and $r > 200-250$ for 6SBD) results in complete resolubilization of the SBD/DNA adducts. This phenomenon is analogous to the well-known salting-in effect of proteins. Resolubilization of DNA by an excess of polyamines or other cationic polymers has been recently described in detail.[25,26] The DNA resolubilization process is easily monitored through CD and absorption spectroscopies and corresponds to the saturation conditions detected by EPR. Absorption spectra show reappearance of a weak band in the 280−300 nm range for 2SBD at $r > 100$. Most remarkably, CD spectra show inversion of the positive band at 270 nm, which reaches its maximum intensity for $r = 200$. In the case of 6SBD the CD spectrum of DNA is progressively recovered with the increase of $r$ ($r > 200-250$) and, at the highest ratios, undergoes characteristic modifications. At $r = 800$, the spectrum exhibits a very strong hyperchromic effect accompanied by spectral shape changes. (The positive and negative bands increase by a factor ~3, and the negative band assumes a much narrower shape.) It is noteworthy that the CD bands are not shifted, as was found for a similar system by Arigita et al.[26] The absence of the shift in wavelength in our spectra indicates that the structural variations, responsible for the hyperchromic effect we found, do not modify the DNA secondary structure from B to C. Furthermore, this conformational change is not permanent: the interaction is essentially reversible, and by adding more SBD to dendrimer/DNA adducts at high ratios, DNA restores its correct folding. Therefore, we suppose that the delivery of DNA to cells by the dendrimers is not compromised by this conformational change.

On passing from $r = 100$ to $r = 200$, the absorption spectrum shows the sudden appearance of an intense band at 260 nm. This band is assigned to redissolved DNA; the unusual form of this band is probably due to important absorption contributions from the binding dendrimer. Overall, we take such strong CD and UV effects, together with the occurrence of a further broad maximum of the EPR parameter as evidence for the formation of soluble SBD/DNA supramolecular structures in which several dendrimers are linked to each DNA molecule, as described in Scheme 2. Notably, occurrence of DNA melting under these extreme conditions is evidence for the conservation of the double-stranded structure, even if the melting process appears to be highly perturbed.

It is of particular interest to analyze the EPR behavior of SBD/DNA complexes which occur at high values of $r$. The EPR spectra of SBD/DNA samples within this range exhibit some interesting features. The peaks observed in the graphs at $r = 100$ in the case of 2SBD-T and $r = 200$ in the case of 6SBD-T (see Figure 5) most likely correspond to formation of supramolecular adducts for which the DNA double helix heavily coats the dendrimers (Scheme 2). It is noteworthy that this saturation condition corresponds to the beginning of the recovery of the CD and UV spectra at high $r$. From the EPR data, formation of these supramolecular structures is accompanied by a net decrease in label mobility, although the decrease in mobility is comparable to that observed upon formation of the low-solubility aggregates. This saturation condition revealed by EPR occurs at lower $r$ values for 2SBD-T with respect to 6SBD-T and is in line with a stronger interacting ability of the smaller dendrimer.

The maximum at $r = 200$ for 6SBD allowed a rough but informative calculation of the stability constant for the formation of supramolecular adducts constituted by DNA wrapping around 6SBD, such as it does with the histones. We took the following into consideration: (a) reduction in the EPR signal intensity upon the freezing transition of the solutions (about 30% of the initial amount remains to contribute to the EPR signal for a SBD concentration of 0.01 M in surface groups; surprisingly this percentage almost does not change in a $r$ range between 100 and 600); (b) the maximum at $I_s/I_f = 1.4$ (60% of the remaining labels interacting with DNA); (a) + (b) provides a resulting dendrimer concentration (in external sites) of [6SBD-T] $\approx 2 \times 10^{-3}$ M; (c) the so-called DNA-linker corresponding, in analogy with the DNA−histone adducts, to 20% of DNA sites is not involved in the interaction;[27] therefore, the resulting DNA concentration (in base pairs) is about $4 \times 10^{-5}$ M; (d) as is commonly accepted, DNA forms two loops around the histone molecules.[27] On the basis of the

analogy with the DNA/histone complex, as reported in the literature,[27] the DNA−6SBD interaction involves 120 base pairs of DNA and about 80 surface groups of 6SBD-T. Therefore, the resulting concentration of the DNA−6SBD adduct is about $3 \times 10^{-5}$ M.

On the basis of these observations, the equilibrium constant for the reaction: 6SBD (surface groups) + DNA (base pairs) = 6SBD−DNA is roughly calculated as $K = 1.5 \times 10^3$ $M^{-1}$. The accuracy in this binding constant is very low (about 40%) but still provides confirmation of the stability of the SBD−DNA adducts. A similar calculation for 2SBD was not made because we do not have a basis for estimating the formation of loops of DNA and consequent formation of DNA-linker.

Interestingly, without buffer, no precipitation is observed; accordingly, the peaks located around $r = 100$ and $r = 200$ are not present (Figure 6). The resulting profile is far more regular, exhibiting a progressive decrease in mobility upon increasing $r$ until a plateau or a broad maximum is reached. This behavior most likely reflects progressive formation of highly structured adducts. The absence of saturation peaks at low $r$ values was mainly due to the pH conditions (pH at about 8.5−9) which prevent the neutralization and precipitation of the DNA/SBD adducts with the consequent opalescence of the solution. The saturation in the absence of the buffer corresponds to the broad peak of EPR mobility found at very high $r$ values ($r = 500-600$ for 2SBD-T and $r = 700-800$ for 6SBD-T). The formation of unusual supramolecular structures in this range of $r$ values, both in the absence and in the presence of the buffer, is also demonstrated by some CD, UV, and melting profile features, such as the inversion of the CD adsorption for 2SBD, the significant hyperchromic effect for 6SBD, the shift of the UV adsorptions, and the strong perturbation of the melting profiles.

Finally, the apparent stronger DNA interactions of 2SBD compared to 6SBD deserves consideration. We propose that the fluid open structure of the small dendrimers adapts well to the DNA surface, whereas the DNA forms loops around the large dendrimers (in analogy with the wrapping of DNA around the histones).

## Conclusions

The results of CD, UV, melting point profiles, and EPR analysis allowed the construction of a model for the structures and interactions of starburst dendrimers with calf thymus DNA as a function of the SBD/DNA ratio (Scheme 2). These results are of interest because of the potential that SBDs have shown to be specific transfection agents for genetic material. The main findings of this study are reported below.

(i) At low ratios of [SBD]/[DNA] both 2SBD and 6SBD give rise to rather strong electrostatic interactions with DNA. Small structural modifications of B-type DNA conformation result. Few SBD molecules are interacting with DNA (Scheme 2).

(ii) At intermediate ratios of [SBD]/[DNA], the neutralization of DNA negative charge by SBDs leads to precipitation and subsequent opalescence of the solution up to $r = 100$ for 2SBD and $r = 200$ for 6SBD. Variation in CD and UV spectra and the occurrence of a maximum in interaction detected by EPR are consistent with the formation of supramolecular structures constituted by aggregates of DNA and SBD molecules (Scheme 2).

(iii) At high ratios of [SBD]/[DNA], the SBDs are able to resolubilize DNA completely due to a salting-in effect. For both dendrimers EPR shows the occurrence of a further broad maximum in the DNA−SBD interactions, whereas CD, UV, and melting profiles indicate variations (but reversible) of the DNA structure. The results are explained in terms of the formation of supramolecular structures in which several dendrimers bind to DNA (Scheme 2).

(iv) Finally, some significant differences in DNA interactions were detected between 2SBD and 6SBD that most likely arise from the fact that 2SBD is far smaller and has a more fluid structure with respect to 6SBD and therefore better fits DNA conformation (Scheme 2).

Overall, these results clearly demonstrate that poly(amidoamine) dendrimers of different generation are able to bind calf thymus DNA. This behavior is easily explained on the basis of the occurrence of strong electrostatic interactions between the positively charged groups located on the surface of the dendrimers and the negative phosphate groups of DNA. This study suggests that adducts of different stoichiometries may be prepared to be used in gene delivery strategies. It is remarkable that the SBD/DNA interactions, here investigated, although relatively tight, are electrostatic in nature and reversible; this implies that such adducts should not modify permanently DNA structure and function. If these adducts turn out to be sufficiently stable under physiological conditions, far different results in terms of selectivity, biodistribution, and DNA delivery efficiency may result.

**Acknowledgment.** M.F.O. thanks the Italian Ministero dell' Università e della Ricerca Scientifica (MURST) for the financial support. The authors thank Dr. Wei Chen for the characterization of the DNA solutions and Monica Manetti for help in recording the EPR spectra. L.M. thanks the Cassa di Risparmio di Firenze for a generous grant. Support by the consortia CIBIACI and CIRCMSB is gratefully acknowledged. The authors at Columbia thank the NSF for support of this research through Grant CHE98-12878; this work was supported in part by the MRSEC Program of the National Science Foundation under Award DMR-98-09687.

## References and Notes

(1) *Advances in Dendritic Macromolecules*; Newkome, G. R., Ed.; JAI Press: Greenwich, CT, 1993. (b) Newkome, G. R.; Moorefield, C. N.; Baker, G. R.; Johnson, A. L.; Behera, R. K. *Angew. Chem., Int. Ed. Engl.* **1991**, *30*, 1176. (c) Makelburger, H. B.; Jaworek, W.; Vögtle, F. *Angew. Chem., Int. Ed. Engl.* **1992**, *31*, 1571. (d) Issberner, J.; Moors, R.; Vögtle, F. *Angew. Chem., Int. Ed. Engl.* **1994**, *33*, 2413. (e) Alper, J. *Science* **1991**, *251*, 1562. (f) Krohn, K *Org. Synth. Highlights* **1991**, 378. (g) Amato, L. *Sci. News* **1990**, *138*, 298. (h) Kim, Y. H.; Webster, O. W. *J. Am. Chem. Soc.* **1990**, *112*, 4592. (i) Hawker, C. J.; Wooley, K. L.; Fréchet, J. M. J. *J. Chem. Soc., Perkin Trans. 1* **1993**, 1287. (j) Fréchet, J. M. J. *Science* **1994**, *263*, 1710.

(2) Tomalia, D. A.; Hall, M.; Hedstrand, D. M. *J. Am. Chem. Soc.* **1987**, *109*, 1601. (b) Tomalia, D. A.; Naylor, A. M.; Goddard, W. A., III *Angew. Chem., Int. Ed. Engl.* **1990**, *29*, 138. (c) Tomalia, D. A.; Durst, H. D. In *Topics in Current Chemistry*; Weber, E., Ed.; Springer-Verlag: Berlin, 1993; Vol. 165, p 193.

(3) Bielinska, A. U.; Chen, C.; Johnson, J.; Baker, J. R. *Bioconjugate Chem.* **1999**, *10*, 843.

(4) Haensler, J.; Szoka, F. C. *Bioconjugate Chem.* **1993**, *4*, 372.

(5) (a) Kukowska-Latallo, J. F.; Bielinska, A. U.; Johnson, J.; Spindler, R.; Tomalia, D. A.; Baker, J. R. *Proc. Natl. Acad. Sci. U.S.A.* **1996**, *93*, 4897. (b) Bielinska, A. U.; Kukowska-Latallo, J. F.; Johnson, J.; Tomalia, D. A.; Baker, J. R. *Nucleic Acids Res.* **1996**, *24*, 2176.

(6) Kim, Y.; Zimmerman, S. C. *Curr. Opin. Chem. Biol.* **1998**, *2*, 733.
(7) Gonzales, H.; Hwang, S. J.; Davis, M. E. *Bioconjugate Chem.* **1999**, *10*, 1068.
(8) Godbey, W.; Wu, K.; Hirasaki, G.; Mikos, A. *Gene Ther.* **1999**, *6*, 1380.
(9) Bosman, A. W.; Janssen, H. M.; Meijer, E. W. *Chem. Rev.* **1999**, *99*, 1665.
(10) Shchepinov, M. S.; Udalova, I. A.; Bridgman, A. J.; Southern, E. M. *Nucleic Acids Res.* **1997**, *25*, 4447.
(11) Bielinska, A. U.; Kukowska-Latallo, J. F.; Baker, J. R. *Biochim. Biophys. Acta* **1997**, *1353*, 180.
(12) Tang, M. X.; Redemann, C. T.; Szoka, F. C. *Bioconjugate Chem.* **1996**, *7*, 703.
(13) Turunen, M. P.; Hiltunen, M. O.; Ruponen, M.; Virkamaki, L.; Szoka, F. C.; Yla-Herttuala, S. *Gene Ther.* **1999**, *6*, 6.
(14) Holter, W.; Fordis, C. M.; Howard, B. H. *Exp. Cell Res.* **1999**, *184*, 546.
(15) Kukowska-Latallo, J. F.; Chen, C.; Eichman, J.; Bielinska, A. U.; Baker, J. R. *Biochim. Biophys. Res. Commun.* **1999**, *264*, 253.
(16) (a) Ottaviani, M. F.; Daddi, R.; Brustolon, M.; Turro, N. J.; Tomalia, D. A. *Langmuir* **1999**, *15*, 1973. (b) Ottaviani, M. F.; Matteini, P.; Brustolon, M.; Turro, N. J.; Jockusch, S.; Tomalia, D. A. *J. Phys. Chem. B* **1998**, *102*, 6029.
(17) Ottaviani, M. F.; Sacchi, B.; Turro, N. J.; Chen, W.; Jockusch, S.; Tomalia, D. A. *Macromolecules* **1999**, *32*, 2275.
(18) Chen, W.; Turro, N. J.; Tomalia, D. A. *Langmuir* **2000**, *16*, 15.
(19) Wilson, W. D.; Tanios, F. A.; Fernandez-Saiz, M.; Rigl, C. T. In *Methods in Molecular Biology;* Fox, K. R., Eds.; Humana Press: Totowa, NJ, 1997; Vol. 90.
(20) Haroutiunian, S. G.; Dalyan, E. B.; Aslanyan, V. M.; Lando, D. Y.; Akhrem, A. A. *Nucleic Acids Res.* **1990**, *18*, 21.
(21) Naylor, A. M.; Goddard, W. A., III; Kiefer, G. E.; Tomalia, D. A. *J. Am. Chem. Soc.* **1989**, *111*, 2341.
(22) Ottaviani, M. F.; Montalti, F.; Romanelli, M.; Turro, N. J.; Tomalia, D. A. *J. Phys. Chem.* **1996**, *100*, 11033.
(23) (a) *Spin Labeling. Theory and Applications*; Berliner, L. J., Ed.; Academic Press: New York, 1976, Vol. 1; 1979, Vol. 2. (b) *Biological Magnetic Resonance. Spin Labeling. Theory and Applications*; Berliner, L. J., Reuben, J., Eds.; Plenum Press: New York, 1989; Vol. 8.
(24) Schneider, D. J.; Freed, J. H. In *Biological Magnetic Resonance. Spin Labeling. Theory and Applications*; Berliner, L. J., Reuben, J., Eds.; Plenum Press: New York, 1989; Vol. 8.
(25) Saminathan, M.; Antony, T.; Shirahata, A.; Sigal, L. H.; Thomas, T.; Thomas, T. J. *Biochemistry* **1999**, *38*, 3821.
(26) Arigita, C.; Zuidam, N. J.; Crommelin, D. J. A.; Hennink, W. E. *Pharm. Res.* **1999**, 1534.
(27) Rawn, J. D. *Biochimica*; McGraw-Hill: Milano, Italy, 1990.

MA000877I